Available online at www.sciencedirect.com
ScienceDirect
Medical Engineering & Physics 30 (2008) 834–842
Medical Engineering & Physics
www.elsevier.com/locate/medengphy

Enhancement of accuracy and reproducibility of parametric modeling for estimating abnormal intra-QRS potentials in signal-averaged electrocardiograms

Chun-Cheng Lin *

Department of Electrical Engineering, National Chin-Yi University of Technology, No. 35, Lane 215, Section 1, Jhongshan Road, Taiping, Taichung County 411, Taiwan

Received 16 February 2007; received in revised form 28 September 2007; accepted 1 October 2007

Abstract

This work analyzes and attempts to enhance the accuracy and reproducibility of parametric modeling in the discrete cosine transform (DCT) domain for the estimation of abnormal intra-QRS potentials (AIQP) in signal-averaged electrocardiograms. One hundred sets of white noise with a flat frequency response were introduced to simulate the unpredictable, broadband AIQP when quantitatively analyzing estimation error. Further, a high-frequency AIQP parameter was defined to minimize estimation error caused by the overlap between normal QRS and AIQP in low-frequency DCT coefficients. Seventy-two patients from Taiwan were recruited for the study, comprising 30 patients with ventricular tachycardia (VT) and 42 without VT. Analytical results showed that VT patients had a significant decrease in the estimated AIQP. The global diagnostic performance (area under the receiver operating characteristic curve) of AIQP rose from 73.0% to 84.2% in lead Y, and from 58.3% to 79.1% in lead Z, when the high-frequency range fell from 100% to 80%. The combination of AIQP and ventricular late potentials further enhanced performance to 92.9% (specificity = 90.5%, sensitivity = 90%). Therefore, the significantly reduced AIQP in VT patients, possibly also including dominant unpredictable potentials within the normal QRS complex, may be new promising evidence of ventricular arrhythmias.

Keywords: Signal-averaged electrocardiogram; Ventricular late potentials; Abnormal intra-QRS potentials; Discrete cosine transform; Parametric modeling

1. Introduction

The non-invasive signal-averaged electrocardiogram (SAECG) has, in recent years, became a conventional means of assessing the risk of ventricular arrhythmias [1–3]. If the ventricular arrhythmias can be detected correctly in advance in conjunction with early alarms and appropriate medical treatments, then the threat of sudden cardiac death can be reduced effectively. During the past decades, SAECG analysis has concentrated on the ventricular late potentials (VLP), which are linked to the development of ventricular tachycardia (VT). Previous studies [2,3] have shown that time-domain analysis for VLP detection has the benefits of high reproducibility and excellent negative predictive accuracy when differentiating the true negative subjects from those with a negative result. However, regarding positive predictive accuracy, the proportion of correctly diagnosed patients with positive results was insufficient to justify intervention in patients with abnormal results. Although many other transform domain approaches have been devoted to improving the performance of VLP detection [4–10], no consensus yet exists on their methods and clinical applications [11,12].

To enhance the diagnostic performance of SAECG, a new index, named abnormal intra-QRS potentials (AIQP), which originates inside the QRS complex, has been presented by Gomis et al. [13] and Lander et al. [14] to measure the risk of ventricular arrhythmias. They developed a parametric model in the discrete cosine transform (DCT) domain to estimate the AIQP. Their study results [13,14] demonstrated that AIQP can be applied to diagnose the risk of ventricular arrhythmias. The AIQP parameter has also been applied to identify the mechanisms of premature ventricular beats

* Tel.: +886 4 2392 4505x7238; fax: +886 4 2392 4419.
E-mail address: cclin@mail.ncut.edu.tw.

1350-4533/$ – see front matter © 2007 IPEM. Published by Elsevier Ltd. All rights reserved.
doi:10.1016/j.medengphy.2007.10.001

(PVB) [15]. The sinus beats immediately preceding the PVB reportedly exhibit significant change. The study of Lander et al. [16] further reported that AIQP changes are apparently more sensitive for detecting acute transmural ischemia than QRS or ST-segment changes in the standard 12-lead ECG.

However, the main limitation of the AIQP extraction methodology is that selecting the critical model order depends on the clinical data [13]. Although the cross-correlation method [17] provides a basis for the model order selection, it cannot confirm that the chosen model order is accurate because the true model order is unknown for practical AIQP estimations. Hence, the uncertainty of the selected model order would result in an unavoidable error for AIQP estimation.

The particular feature of the DCT-domain parametric model is that the input signal can be transformed by DCT to a real frequency-domain signal, rather than a complex one. Since most energy of the smooth, predictable QRS complex is concentrated in the low-frequency band, a low-order model can be employed to estimate the normal QRS complex and then separate out the low-amplitude, broadband, unpredictable AIQP. However, the overlap between the normal QRS complex and AIQP in the low-frequency band may cause a high AIQP estimation error even if the selected model order is accurate. Previous studies did not address this problem.

This investigation introduces 100 independent sets of white noise to simulate the broadband, unpredictable AIQP. Simulation results indicate that the estimated AIQP has obvious estimation errors in the low-frequency DCT coefficients, due to the overlap of the normal QRS complex and AIQP in the DCT-domain low-frequency band. In order to improve the accuracy of AIQP analysis, this study eliminates some low-frequency DCT coefficients with estimation errors to define a high-frequency AIQP parameter. The aim of this work is to enhance the accuracy, reproducibility and clinical performance of the AIQP parameter using DCT-domain parametric modeling.

2. Methods

2.1. Data acquisition

This study followed the principles that (1) informed consent was obtained from each patient and (2) the Ethics Committee of Taipei Jen-Chi General Hospital has approved the study. High-resolution ECGs were obtained from 72 subjects. The methods are described elsewhere [15]. The subjects were divided into two groups. Group I (normal group) comprised 42 normal Taiwanese (20 men and 22 women, aged 58 ± 14 years old). All individuals had a normal clinical history, physical examination, 12-lead ECG, and echocardiogram. Group II (VT group) consisted of 30 patients (15 men and 15 women, aged 63 ± 16 years old) with sustained VT documented by 24-h Holter ECG monitoring. They suffered from chronic ischemic heart disease surviving clinically documented myocardial infarction.

Signal averaging was performed to lower the effects of random noise [2,3]. The final noise level of SAECG measured by a bidirectional Butterworth filter with a 40–250 Hz bandpass was less than 0.7 μV. The onset and offset of the QRS complex were obtained from vector magnitude analysis. Three standardized time-domain SAECG parameters, namely (1) filtered total QRS duration (fQRSD), (2) RMS voltage of the last QRS 40 ms (RMS40) and (3) duration of the low amplitude signals below 40 μV (LAS40), were adopted to detect VLP.

2.2. Parametric modeling for evaluating abnormal intra-QRS potentials

Our previous study [17] has proposed an autoregressive moving average (ARMA) model in the DCT domain as illustrated in Fig. 1, comprising M sets of ARMA (2, 2) model, to estimate the smooth, predictable QRS complex and then separate out the unpredictable AIQP. The input QRS complex $x(n)$ was assumed to be composed of the normal QRS complex $s(n)$ and AIQP $v(n)$. The input signal was first transformed using DCT to a set of real frequency-domain signals. The corresponding signals in the DCT domain were $X(k)$, $S(k)$ and $V(k)$.

The transfer function of the ARMA ($2M$, $2M$) model in the DCT domain is defined as follows [17,18]:

$$H(z^{-1}) = \frac{B_0 + B_1 z^{-1} + \cdots + B_{2M} z^{-2M}}{1 + A_1 z^{-1} + \cdots + A_{2M} z^{-2M}} \quad (1)$$

where $A_1, A_2, \ldots, A_{2M}$ and $B_0, B_1, \ldots, B_{2M}$ are the model coefficients. The modeling output $\hat{S}(k)$ was employed to estimate the normal QRS complex. Given a specific model order M, the iterative least squares error algorithm of Steiglitz and McBrige [19] was introduced to estimate the optimal model coefficients. The modeling residual $\hat{V}(k)$ was adopted to estimate AIQP. The estimated normal QRS complex $\hat{s}(n)$ and AIQP $\hat{v}(n)$ in the time domain can be derived through the inverse discrete cosine transform (IDCT). The cross-correlation coefficient ρ between the modeling output $\hat{s}(n)$ and the desired input $x(n)$ was employed to evaluate the estimation accuracy of the normal QRS complex [17]. The optimal model order was defined to reach a predetermined threshold of the cross-correlation coefficient [17]. The high-frequency AIQP parameter, AIQP_l(q%), is defined in Section 2.4.

2.3. Accuracy analysis for the estimation of abnormal intra-QRS potentials

Because of the broadband and unpredictable characteristics of AIQP, this study introduced normally distributed white noise [20] consisting of a random process with a flat fre-

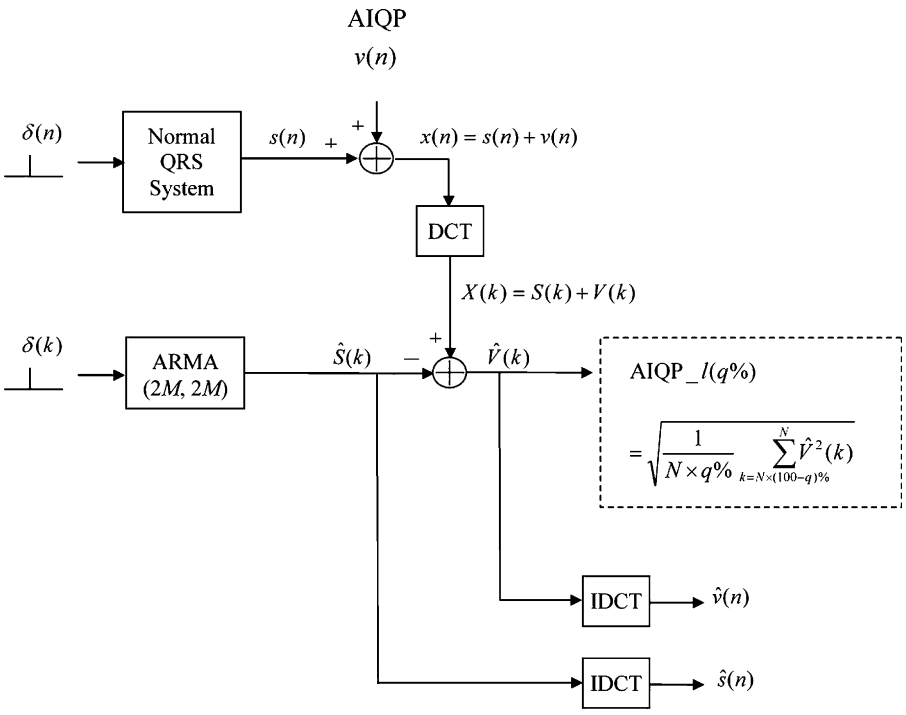

Fig. 1. Block diagram of parametric modeling in discrete cosine transform domain for AIQP estimation. AIQP, abnormal intra-QRS potentials; ARMA, autoregressive moving average; DCT, discrete cosine transform; IDCT, inverse DCT.

quency response and a probability density function of normal distribution (also known as Gaussian distribution) to simulate AIQP for quantitative analysis of the estimation error. Further, since the true model order of a practical QRS complex is unknown, an ARMA (6, 6) QRS complex extracted from lead X of a normal subject was selected in order to simulate the normal QRS complex (Fig. 2(a)). The peak-to-peak amplitude is about 1500 μV, and the QRS duration is 106 ms. Fig. 2(b) displays a set of normally distributed white noise with zero mean to simulate AIQP. The signal-to-noise ratio (SNR) is only −40 dB (AIQP versus the normal QRS complex).

Fig. 3(a) and (b) illustrates the modeling outputs (solid line) estimated using the true model order (6, 6) in the DCT-domain and time-domain, respectively, where the dotted lines denote the true normal QRS complex. The small estimation error is hard to observe from the figure, owing to the high amplitude of the QRS complex. Fig. 3(c) and (d) depicts the modeling residuals (solid line) in the DCT domain and time-domain, respectively. A noticeable estimation error occurred in the DCT-domain low-frequency band when comparing the modeling residual with the true AIQP (dotted line) (Fig. 3(c)). In the time-domain, the estimation error was sustained in the entire QRS (Fig. 3(d)).

The AIQP estimation errors in the DCT-domain and time-domain, calculated as the differences between the true and estimated AIQP, are shown in Fig. 4(a) and (b), respectively. Clearly, most of the estimation errors occurred in the DCT-domain low-frequency band and were approximately 30% of the total DCT coefficients (k = 1–32) (Fig. 4(a)). The corresponding estimation error of AIQP in the time domain was a low-frequency wave (Fig. 4(b)).

Notably, the existing AIQP would influence the estimation accuracy even if a true model order was used. This is because of the overlap of the normal QRS complex and AIQP in the DCT domain, especially in the low-frequency band in which most of the normal QRS complex is concentrated. Therefore, the estimation of the normal QRS complex is inevitably involved with some low-frequency AIQP.

2.4. Definition of the high-frequency AIQP parameter

To improve the accuracy of the AIQP estimation, this investigation disregarded the low-frequency coefficients with estimation errors, and only utilized high-frequency DCT coefficients to define the AIQP parameter. The high-frequency AIQP parameter was defined as follows:

$$\text{AIQP\_l}(q\%) = \sqrt{\frac{1}{N \times q\%} \sum_{k=N\times(100-q)\%}^{N} \hat{V}^2(k)} \qquad (2)$$

where $q\%$ indicates the percentage of the total DCT coefficients for the analysis of the high-frequency AIQP, N denotes the QRS duration, and l represents the lead X, Y or Z. No DCT coefficient is ignored when $q\% = 100\%$. Although reducing $q\%$ can raise the accuracy of the high-frequency AIQP, it may decrease the clinical performance due to losing

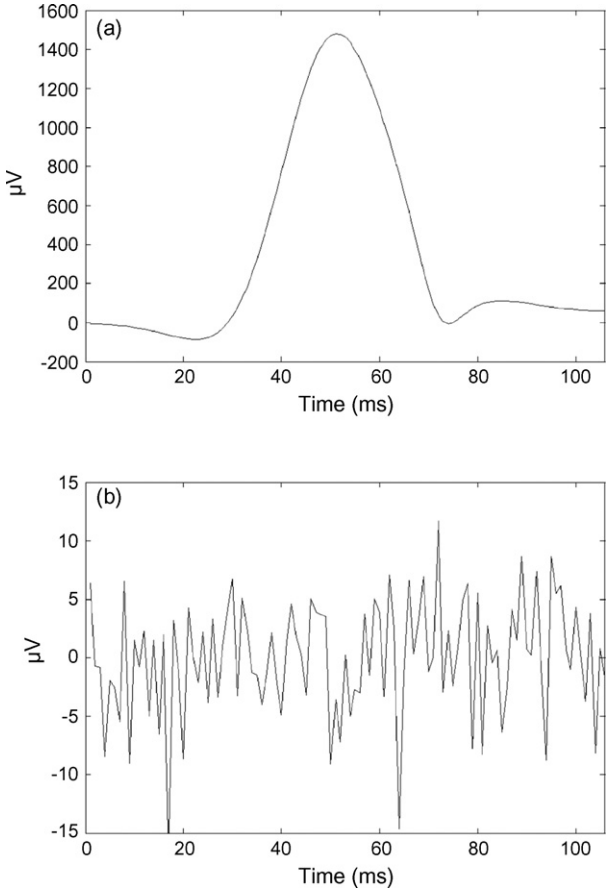

Fig. 2. Simulation signals: (a) an ARMA (6, 6) signal simulating normal QRS complex; (b) a normally distributed white noise with zero mean simulating AIQP.

too many low-frequency features. Hence, the choice of $q\%$ is a compromise between estimation accuracy and clinical performance.

2.5. Statistical methods

All statistical analyses were undertaken using Statistical Package for the Social Sciences®. The F-test was utilized to compare the variances of different variables, and the Student's t-test with two tails was adopted to compare the means of two independent variables. Statistical significance was defined as $p < 0.05$. Pearson's product moment correlation coefficient was employed to measure the level of linear correlation. The local performance indices used in this study were specificity, sensitivity, positive predictive accuracy (PPA), negative predictive accuracy (NPA) and total predictive accuracy (TPA) [21]. The receiver operating characteristic (ROC) curve was applied to analyze the global diagnostic performance and as a reference for specifying the local threshold [22,23]. The area under the ROC curve (AUC) was utilized as an index for evaluating the global performance.

3. Results

3.1. Simulation results for the analysis of accuracy and reproducibility of the high-frequency AIQP parameter

This study used 100 independent sets of normally distributed white noise with zero mean to simulate the broadband, unpredictable AIQP, and to analyze the accuracy and reproducibility of the high-frequency AIQP parameter. The AIQP was estimated under different values of $q\%$ (100%, 90% and 80%) and magnitudes (AIQP_|($q\%$) = 0–10 μV). The normal QRS complex was simulated by an identical ARMA (6, 6) signal of leading X in Fig. 2(a).

Fig. 5(a)–(c) is the simulation results of true versus estimated AIQP_X($q\%$) for $q\%$ values of 100%, 90% and 80%, respectively. Each curve corresponds to a set of white noise under different AIQP magnitudes (AIQP_X($q\%$) = 0–10 μV). Simulation results demonstrate that a lower $q\%$ indicates less dispersive curves, and better accuracy and reproducibility. The percentage of the estimation error for each AIQP estimation result was determined further as follows:

$$E\ (\%) = \left|\frac{\text{estimated} - \text{true}}{\text{true}}\right| \times 100\% \quad (3)$$

Fig. 5(d)–(f) shows the average percentages of the estimation errors of all magnitudes (AIQP_X($q\%$) = 0–10 μV) versus 100 sets of white noise for $q\%$ values of 100%, 90% and 80%, respectively. These figures clearly reveal that a lower $q\%$ has a lower percentage of estimation error. Moreover, the mean values and standard deviations of the average error percentages were $5.46 \pm 2.14\%$, $1.76 \pm 1.33\%$ and $0.31 \pm 0.38\%$ for $q\%$ values of 100%, 90% and 80%, respectively. A lower $q\%$ following the lower mean value and standard deviation indicates better accuracy and reproducibility of the high-frequency AIQP parameter.

3.2. Clinical results

This study conducted AIQP analysis with different $q\%$ values (100%, 90%, 80%, 70% and 60%) and thresholds of model order selection (cross-correlation coefficient = 0.990–0.999 with a 0.001 interval, and 0.9995, 0.9999) for leads X, Y and Z. Analytical results show that the high-frequency AIQP parameters in leads Y and Z can significantly differentiate between VT and normal groups, but not in lead X. Fig. 6(a) and (b) illustrates the curves of the cross-correlation coefficient threshold ρ versus AUC under various $q\%$ values for the high-frequency AIQP parameters in leads Y and Z, respectively.

The analytical results reveal that the best clinical diagnostic performance (AUC) achieved 84.2% ($q\% = 80\%$, $\rho = 0.998$) and 79.1% ($q\% = 80\%$, $\rho = 0.994$) in leads Y and Z, respectively. The AUC of AIQP increased from 73.0% to 84.2% in lead Y ($\rho = 0.998$), and from 58.3% to 79.1% in lead Z ($\rho = 0.994$), when $q\%$ decreased from 100% to 80%, but fell from 84.2% to 73.6% in lead Y, and from 79.1% to

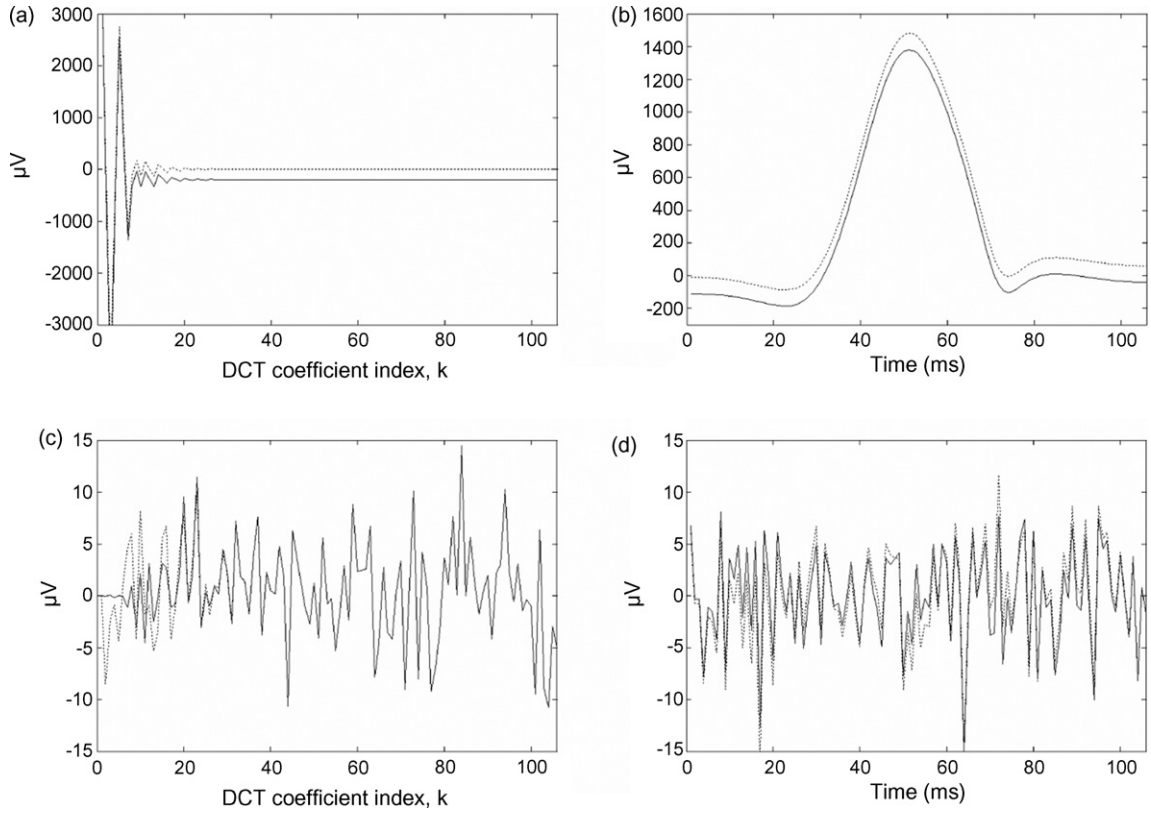

Fig. 3. Simulation results: modeling output in (a) DCT domain and (b) time domain; modeling residual in (c) DCT domain and (d) time domain.

72.1% in lead Z, when q% continuously fell from 80% to 60%.

Table 1 summarizes the time-domain VLP parameters and the high-frequency AIQP parameters, where the cross-correlation thresholds were set at 0.998, 0.998 and 0.994 in leads X, Y and Z, respectively, for AIQP analysis. The results of the time-domain VLP parameters are consistent with several earlier studies [1–3]. Both the mean AIQP_Y(80%) and AIQP_Z(80%) of the VT group were significantly lower than those of the normal group ($p<0.001$). The mean AIQP_X(80%) of the VT group were also lower than that of the normal group, but not significantly so ($p>0.05$). Each SAECG had its own optimum model order, and no significant differences ($p>0.05$) were found in the optimum model order of each lead between the VT and normal groups.

The correlation analysis demonstrated significant correlations ($p<0.05$) between AIQP_Y(80%) and fQRSD ($\rho=-0.39$), RMS40 ($\rho=0.45$) and LAS40 ($\rho=-0.42$), and between AIQP_Z(80%) and RMS40 ($\rho=0.44$) and LAS40 ($\rho=-0.33$). The AIQP parameters were not statistically correlated with gender or age ($p>0.05$).

Table 2 lists the global and local performances of time-domain VLP, high-frequency AIQP and synthesized parameters, where the cross-correlation thresholds were set

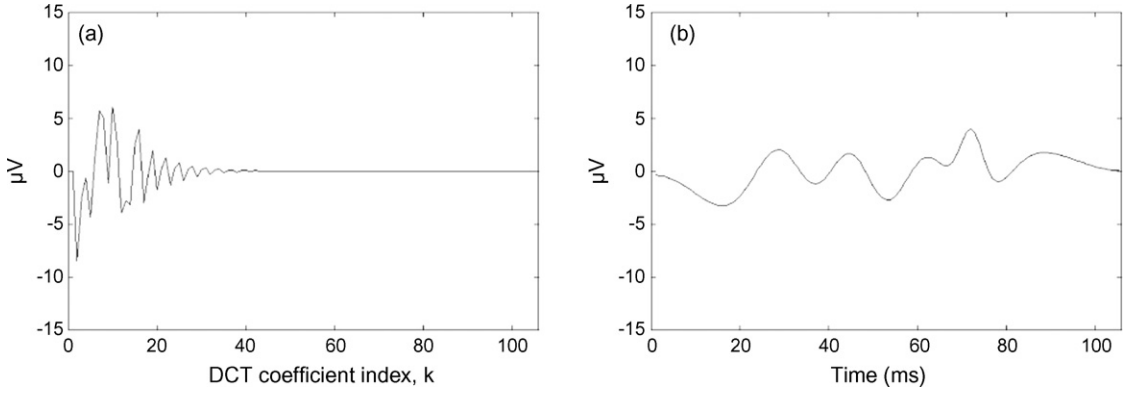

Fig. 4. Estimation errors of AIQP in (a) DCT domain and (b) time domain.

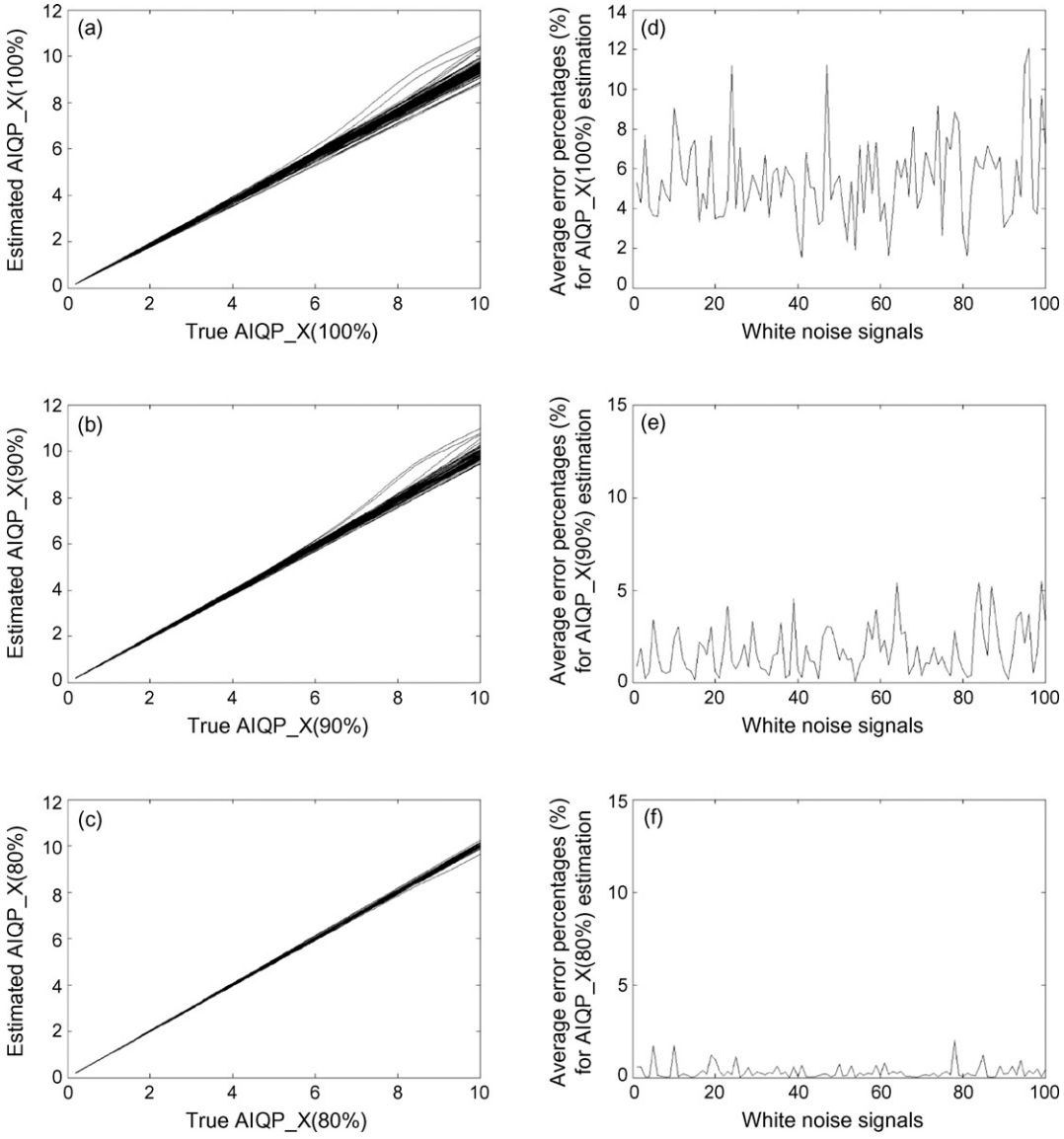

Fig. 5. Simulation results evaluating the estimation accuracy and reproducibility of the high-frequency AIQP parameter: (a)–(c) depict the curves of true vs. estimated values for q% values of 100%, 90% and 80%, respectively; (d)–(f) illustrate the average percentages of the estimation errors of all magnitudes (AIQP_X(q%) = 0–10 μV) vs. 100 sets of white noise for q% values of 100%, 90% and 80%, respectively.

at 0.998, 0.998 and 0.994 in leads X, Y and Z, respectively, for AIQP analysis. Two parameters A and B were linearly combined to synthesize a new parameter $A \times \alpha B$, where the weight of parameter A was fixed at 1, and the optimum value of α was determined to maximize the global performance—that is, to maximize the AUC. The best global performance using the individual parameter was obtained using RMS40 (AUC = 86.7%), and the next best was achieved using AIQP_Y(80%) (AUC = 84.2%). The combination of AIQP_Y(80%) and RMS40 was best (AUC = 92.2%) among all combinations of the two individual parameters. The performance of the synthesized AIQP parameter (AIQP_Y(80%) + 0.4 × AIQP_Z(80%)) was increased to 92.6% of AUC by combining it with RMS40, and to 92.9% by combining it with RMS40 and fQRSD. The analysis of the local performance was at a local operating point with 90.5% specificity to compare sensitivity, PPA, NPA and TPA. The combination of AIQP_Y(80%), AIQP_Z(80%), RMS40 and fQRSD had the best local performance (sensitivity = 90.0%, PPA = 87.1%, NPA = 92.7%, TPA = 90.3%).

4. Discussion and conclusions

4.1. Improvement of accuracy and reproducibility for AIQP estimation

The main contribution of this investigation is to enhance the accuracy and reproducibility for AIQP analysis in the

Table 1
Mean values and standard deviations of time-domain and high-frequency AIQP parameters

Groups	AIQP parameters (Optimum model order, 2M)[a] (μV)			Time-domain parameters		
	AIQP_X(80%)	AIQP_Y(80%)	AIQP_Z(80%)	fQRSD (ms)	RMS40 (μV)	LAS40 (ms)
VT	7.4 ± 4.6 (4 ± 1)	7.3 ± 2.4 (6 ± 2)	9.8 ± 4.7 (4 ± 1)	96.5 ± 7.7	20.1 ± 9.6	37.2 ± 6.7
Normal	8.5 ± 3.0 NS (4 ± 1) NS	13.0 ± 5.7* (5 ± 1) NS	15.3 ± 5.0* (4 ± 1) NS	90.3 ± 10.2*	43.7 ± 25.0*	29.0 ± 5.7*

The cross-correlation thresholds in leads X, Y and Z for AIQP analysis are 0.998, 0.998 and 0.994, respectively.
Student's *t*-test with two tails was performed to compare the means of two independent variables.
NS, non-significant ($p > 0.05$); *$p < 0.001$ compared to VT group.
AIQP_l(*q*%), abnormal intra-QRS potentials in lead l (l is lead X, Y or Z) using *q*% of total discrete cosine transform coefficients toward the high-frequency band.
[a] Optimum model order is presented as (mean ± standard deviation); for example, (4 ± 1) stands for the model order (4, 4) ± (1, 1).

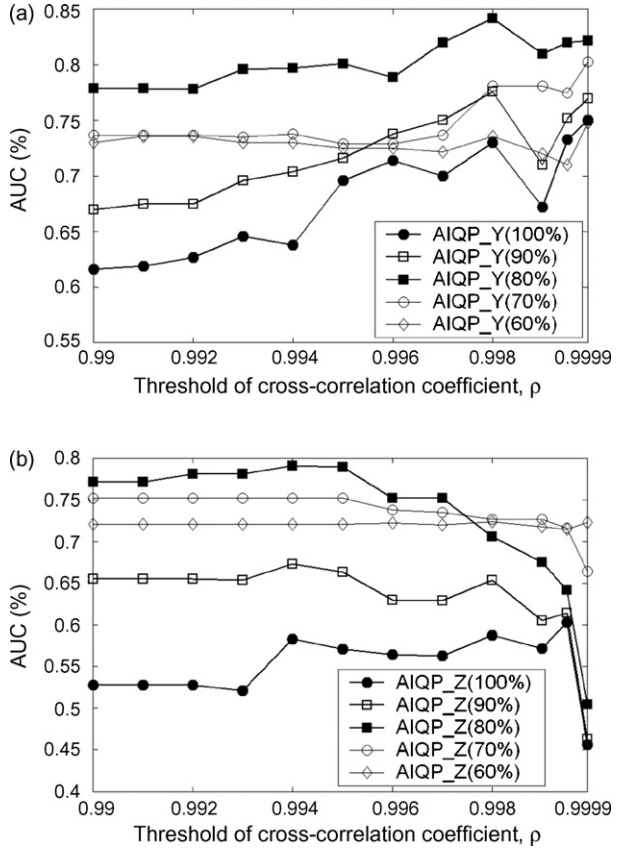

Fig. 6. Performance curves of the cross-correlation coefficient threshold vs. AUC under various *q*% values for the high-frequency AIQP parameters in leads (a) Y and (b) Z. AUC is given by the area under the receiver operating characteristic curve.

DCT-domain parametric modeling. Although previous studies [13,14,17] applied a transient triangular signal to simulate AIQP, they did not further analyze the AIQP estimation accuracy. Since the true frequency band and randomness of AIQP are unknown, this study introduces 100 independent sets of normally distributed white noise with zero mean to simulate the broadband, unpredictable AIQP. The simulation results indicate the poor accuracy and reproducibility of the root-mean-square of the estimated AIQP using DCT domain parametric modeling, which is caused by the estimation error in the low-frequency DCT coefficients. Therefore, this investigation ignores some low-frequency DCT coefficients with estimation errors when defining the high-frequency AIQP parameter. Simulation results show that disregarding more low-frequency DCT coefficients improves the accuracy and reproducibility of the high-frequency AIQP parameter.

4.2. Comparisons with previous studies

Because of the abnormal myocardial conduction, the VT patients were expected to display increased AIQP. However, this work demonstrates that the mean high-frequency AIQP parameters of the VT group in leads Y and Z were significantly lower than those of the normal group ($p < 0.001$), but

Table 2
Global and local performance of time-domain, high-frequency AIQP and synthesized parameters

Parameters	AUC (%)	Specificity = 90.5%			
		Sensitivity (%)	PPA (%)	NPA (%)	TPA (%)
fQRSD	71.4	20.0	60.1	61.3	61.1
RMS40	86.7	63.3	82.6	77.5	79.2
LAS40	81.1	63.3	82.6	77.5	79.2
AIQP_X(80%)	64.2	33.3	71.5	65.5	66.7
AIQP_Y(80%)	84.2	50.0	79.0	71.7	73.6
AIQP_Z(80%)	79.1	53.3	80.0	73.1	75.0
AIQP_Y(80%) + 0.4 × AIQP_Z(80%)	87.3	63.3	82.6	77.5	79.2
AIQP_Y(80%) − 0.1 × fQRSD	87.1	60.0	81,9	76.0	77.8
AIQP_Y(80%) + 0.3 × RMS40	92.2	76.7	85.2	84.5	84.8
AIQP_Y(80%) − 0.5 × LAS40	89.6	73.3	84.6	82.6	83.3
AIQP_Z(80%) − 0.3 × fQRSD	83.5	66.7	83.4	79.2	80.6
AIQP_Z(80%) + 0.7 × RMS40	89.0	73.3	84.6	82.6	83.3
AIQP_Z(80%) − 0.8LAS40	87.9	66.7	83.4	79.2	80.6
AIQP_Y(80%) + 0.4 × IQP_Z(80%) + 0.6 × RMS40	92.6	86.7	86.7	90.5	88.9
AIQP_Y(80%) + 0.4 × IQP_Z(80%) + 0.6 × RMS40-0.1 × Fqrsd	92.9	90.0	87.1	92.7	90.3

The cross-correlation thresholds in leads X, Y and Z for AIQP analysis are 0.998, 0.998 and 0.994, respectively. PPA, positive predictive accuracy; NPA, negative predictive accuracy; TPA, total predictive accuracy; AIQP_l(80%), abnormal intra-QRS potentials in lead l (l is lead X, Y or Z) using 80% of total discrete cosine transform coefficients toward the high-frequency band.

that no significant difference occurred in lead X. This result is consistent with our previous study [17], but not with the studies of Gomis et al. [13] and Lander et al. [14]. The clinical inconsistency does not originate from the different methods of model order selection. The same result was obtained in our database even if a fixed model order was used.

Therefore, this database cannot prove the assumption that the normal QRS complex can be estimated exactly with the parametric model. The estimated AIQP would contain all the unpredictable and high-frequency intra-QRS potentials, including normal and abnormal components, on condition that the normal QRS also includes some dominant unpredictable components, especially in an abrupt R wave.

The reduced high-frequency AIQP in VT patients may also be related to the decreased high-frequency components induced by MI and ischemic heart disease. Several previous studies [24–26] have reported that MI reduced the high-frequency components within the QRS complex. Bhargava and Goldberger [27] and Talwar et al. [28] further showed that MI attenuates both low and high-frequency QRS potentials. From a pathophysiological viewpoint, myocardial necrosis leads to a general decrease in electromotive potentials. Reduced high-frequency components have also been associated with ischemic heart disease [29,30]. Pettersson et al. [29] demonstrated that decreased high-frequency RMS measurements (150–250 Hz) during balloon inflation of percutaneous transluminal coronary angioplasty have a sensitivity of 88% for detecting acute coronary artery occlusions, which is higher than the 71% sensitivity of the conventional ST elevation method. Tragardh et al. [30] showed that the summed 12-lead high-frequency (150–250 Hz) components within the QRS interval in patients with ischemic heart disease were significantly smaller than in normal subjects. Hence, MI and ischemic heart disease may cause the reduction of AIQP in VT patients in this study.

4.3. Diagnostic performance of the reduced unpredictable intra-QRS potentials in VT patients

Although the clinical results of the AIQP parameter appeared to be inconsistent, this study shows that the estimated AIQP parameter to represent the total unpredictable intra-QRS potentials can be applied to measure the risk of ventricular arrhythmias, and can be combined with VLP parameters to improve the diagnostic performance of SAECG. The clinical results reveal that disregarding some low-frequency DCT coefficients improves the diagnostic performance of the high-frequency AIQP parameter. However, losing too many low-frequency DCT coefficients would reduce the diagnostic performance instead.

This study also observed significant correlations between AIQP and VLP parameters. A smaller AIQP_Y(80%) and AIQP_Z(80%) tend to indicate a smaller RMS40 and a longer LAS40. The combination of AIQP and VLP parameters further improved the SAECG performance. Therefore, the significant reduction of all unpredictable intra-QRS potentials in VT patients may be new promising evidence of ventricular arrhythmias.

5. Conclusions

This study has successfully demonstrated that the high-frequency AIQP parameter, while neglecting some low-frequency DCT coefficients with estimation errors, can enhance the accuracy, reproducibility and clinical performance of AIQP analysis. Combining AIQP and VLP analyses further improved the diagnostic performance of SAECG. Unlike previous studies, the VT patients in this study showed a significant reduction in AIQP. Therefore, further investi-

gation is required with larger clinical populations to test the usefulness of AIQP.

Acknowledgements

The author would like to thank the National Science Council of the Republic of China, Taiwan, for financially supporting this research under Contract No. NSC95-2221-E-262-001. Staff of the Hemodialysis Unit and patients of the Cardiology Department at Jen-Chi General Hospital are appreciated for their kind assistance and cooperation in this investigation. Dr Ten-Fang Yang of Taipei Medical University (Taipei, Taiwan) is also appreciated for his clinical suggestions and comments.

Conflict of interest

No author had a financial or personal conflict of interest related to this research or its source of funding.

References

[1] Simson MB. Use of signals in the terminal QRS complex to identify patients with ventricular tachycardia after myocardial infarction. Circulation 1981;64:235–42.
[2] Breithardt G, Cain ME, el-Sherif N, Flowers NC, Hombach V, Janse M, et al. Standards for analysis of ventricular late potentials using high-resolution or signal-averaged electrocardiography: a statement by a task force committee of the European Society of Cardiology, the American Heart Association, and the American College of Cardiology. J Am Coll Cardiol 1991;17:999–1006.
[3] Cain ME, Anderson JL, Arnsdorf MF, Mason JW, Scheinman MM, Waldo AL. Signal-averaged electrocardiography. J Am Coll Cardiol 1996;27:238–49.
[4] Lin CC. Improved frequency-domain analysis of ventricular late potentials. Comput Cardiol 2005;32:479–82.
[5] Bonato P, Bettini R, Speranza G, Furlanello F, Antolini R. Improved late potential analysis in frequency domain. Med Eng Phys 1995;17:232–8.
[6] Haberl R, Jilge G, Pulter R, Steinbeck G. Spectral mapping of the electrocardiogram with Fourier transform for identification of patients with sustained ventricular tachycardia and coronary artery disease. Eur Heart J 1989;10:316–22.
[7] Lander P, Albert DE, Berbari EJ. Spectrotemporal analysis of ventricular late potentials. J Electrocardiol 1990;23:95–108.
[8] Lin CC, Yang TF, Chen CM, Yang IF. Spectrotemporal mapping of signal averaged ECG in Taiwanese chronic renal failure patients. Int J Bioelectromagn 2002;4:247–8.
[9] Kelen GJ, Henkin R, Starr AM, Caref EB, Bloomfield D, el-Sherif N. Spectral turbulence analysis of the signal-averaged electrocardiogram and its predictive accuracy for inducible sustained monomorphic ventricular tachycardia. Am J Cardiol 1991;67:965–75.
[10] Lewandowski P, Meste O, Maniewski R, Mroczka T, Steinbach K, Rix H. Risk evaluation of ventricular tachycardia using wavelet transform irregularity of the high-resolution electrocardiogram. Med Biol Eng Comput 2000;38:666–73.
[11] Kulakowski P, Malik M, Odemuyiwa O, Staunton A, Camm AJ. Frequency versus time domain analysis of the signal-averaged electrocardiogram: reproducibility of the spectral turbulence analysis. Pacing Clin Electrophysiol 1993;16:1027–36.
[12] Vazquez R, Caref EB, Torres F, Reina M, Guerrero JA, El-Sherif N. Reproducibility of time-domain and three different frequency-domain techniques for the analysis of the signal-averaged electrocardiogram. J Electrocardiol 2000;33:99–105.
[13] Gomis P, Jones DL, Caminal P, Berbari EJ, Lander P. Analysis of abnormal signals within the QRS complex of the high-resolution electrocardiogram. IEEE Trans Biomed Eng 1997;44:681–93.
[14] Lander P, Gomis P, Goyal R, Berbari EJ, Caminal P, Lazzara R, et al. Analysis of abnormal intra-QRS potentials. Improved predictive value for arrhythmic events with the signal-averaged electrocardiogram. Circulation 1997;95:1386–93.
[15] Berbari EJ, Bock EA, Cházaro AC, Sun X, Sörnmo L. High-resolution analysis of ambulatory electrocardiograms to detect possible mechanisms of premature ventricular beats. IEEE Trans Biomed Eng 2005;52:593–8.
[16] Lander P, Gomis P, Warren S, Hartman G, Shuping K, Lazzara R, et al. Abnormal intra-QRS potentials associated with percutaneous transluminal coronary angiography-induced transient myocardial ischemia. J Electrocardiol 2006;39:282–9.
[17] Lin CC, Chen CM, Yang IF, Yang TF. Automatic optimal order selection of parametric modeling for the evaluation of abnormal intra-QRS signals in signal-averaged electrocardiograms. Med Biol Eng Comput 2005;43:218–24.
[18] Murthy IS, Prasad GS. Analysis of ECG from pole-zero models. IEEE Trans Biomed Eng 1992;39:741–51.
[19] Steiglitz K, McBride LE. A technique for the identification of linear systems. IEEE Trans Autom Control 1965;AC-10:461–4.
[20] Schilling RJ, Harris SL. Fundamentals of digital signal processing using MATLAB®, Toronto, Ontario. Thomson Eng 2005:204–12.
[21] Griner PF, Mayewski RJ, Mushlin AI, Greenland P. Selection and interpretation of diagnostic tests and procedures. Principles and applications. Ann Intern Med 1981;94:557–92.
[22] Metz CE. Basic principles of ROC analysis. Semin Nucl Med 1978;8:283–98.
[23] Zweig MH, Campbell G. Receiver-operating characteristic (ROC) plots: a fundamental evaluation tool in clinical medicine. Clin Chem 1993;39:561–77.
[24] Goldberger AL, Bhargava V, Froelicher V, Covell J, Mortara D. Effect of myocardial infarction on the peak amplitude of high frequency QRS potentials. J Electrocardiol 1980;13(4):367–71.
[25] Goldberger AL, Bhargava V, Froelicher V, Covell J. Effect of myocardial infarction on high-frequency QRS potentials. Circulation 1981;64(1):34–42.
[26] Berkalp B, Baykal E, Caglar N, Erol C, Akgun G, Gurel T. Analysis of high frequency QRS potentials observed during acute myocardial infarction. Int J Cardiol 1993;42(2):147–53.
[27] Bhargava V, Goldberger A. Myocardial infarction diminishes both low and high frequency QRS potentials: power spectrum analysis of lead II. J Electrocardiol 1981;14(1):57–60.
[28] Talwar KK, Rao GS, Nayar U, Bhatia ML. Clinical significance of high frequency QRS potentials in myocardial infarction: analysis based on power spectrum of lead III. Cardiovasc Res 1989;23(1):60–3.
[29] Pettersson J, Pahlm O, Carro E, Edenbrandt L, Ringborn M, Sörnmo L, et al. Changes in high-frequency QRS components are more sensitive than ST-segment deviation for detecting acute coronary artery occlusion. J Am Coll Cardiol 2000;36:1827–34.
[30] Tragardh E, Pahlm O, Wagner GS, Pettersson J. Reduced high-frequency QRS components in patients with ischemic heart disease compared to normal subjects. J Electrocardiol 2004;37:157–62.